Neurobiology of Disease 174 (2022) 105894

Contents lists available at ScienceDirect

Neurobiology of Disease

journal homepage: www.elsevier.com/locate/ynbdi

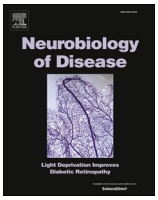

Environmental enrichment counteracts the effects of glioma in primary visual cortex

Maria Amalia Di Castro [a,*], Stefano Garofalo [a], Eleonora De Felice [a], Nicolò Meneghetti [b,c], Erika Di Pietro [a], Alessandro Mormino [a], Alberto Mazzoni [b,c], Matteo Caleo [d], Laura Maggi [a,1], Cristina Limatola [e,f,1,**]

[a] Department of Physiology and Pharmacology, Sapienza University of Rome, Italy
[b] Computational Neuroengineering Laboratory, The Biorobotics Institute, Scuola Superiore Sant'Anna, Pisa, Italy
[c] Department of Excellence in Robotics and AI, Scuola Superiore Sant'Anna, Pisa, Italy
[d] Department of Biomedical Sciences, University of Padua, Italy
[e] Department of Physiology and Pharmacology, Sapienza University, Laboratory affiliated to Istituto Pasteur Italia, Rome, Italy
[f] IRCCS Neuromed Via Atinese 18, 86077 Pozzilli, Italy

ARTICLE INFO

Keywords:
Peritumoral neurons
Glioma
Synaptic transmission
Environmental enrichment

ABSTRACT

Experience-dependent neuronal changes and brain plasticity occur throughout life as animals adapt to their environment. Structural, morphological, and cellular modifications promoted by exposure to environmental enrichment (EE) have been reported to improve neuronal functions, increase hippocampal neurogenesis, ameliorate memory tasks and cognitive performance, and have beneficial effects on several brain diseases, including cancer. We specifically addressed the role of the EE in counteracting neuronal dysfunction in mice bearing glioma in the primary visual cortex. By recording spontaneous and evoked currents with patch clamp techniques in acute slices obtained from standard and enriched-housed mice, we found that the presence of glioma globally reduced the excitatory and inhibitory transmissions in the peritumoral area. The exposure to an enriched environment counteracts the tumor-mediated depression of both excitatory and inhibitory neuronal activities, with a more pronounced impact on evoked transmission. The effect of EE on glioma was also associated with reduced tumor cell proliferation. These results elucidate the impact of EE on excitatory and inhibitory neurotransmission of the primary visual cortex in control and glioma-bearing mice.

1. Introduction

Glioblastoma (GBM) is a high-grade glioma with few therapeutic options for patients. The rapid growth of glioma is regulated by cellular mechanisms intrinsic to cancer cells, but also by bidirectional communication among the different cell populations of brain parenchyma that, together with resident and infiltrating immune cells, take part in the definition of the tumor microenvironment (Cuddapah et al., 2014). Glioma cell proliferation is favored by a permissive and immunosuppressed host environment, induced by soluble and membrane bound tumor-derived factors that weaken or abolish the anti-tumor, immune defense mechanisms (Razavi et al., 2016; Daubon et al., 2020). New emerging studies suggest that glioma cell interaction with neurons and the effects of neuronal activity are critical factors in determining glioma fate (Jung et al., 2019). Neuronal activity promotes the growth and progression of glioma through the secretion of soluble factors such as Neuroligin 3, which affects cell proliferation and invasion capability (Venkatesh et al., 2015; Venkatesh et al., 2017; Venkataramani et al., 2019). Previously it was demonstrated that glioma cells release high levels of glutamate, leading to AMPA and Ca^{2+} permeable NMDA receptors activation, and neuronal hyperexcitability (Buckingham et al., 2011; Campbell et al., 2012). Glioma-mediated neuronal overexcitation and excitotoxicity reduce the viability of the GABAergic interneurons and alter the levels of neuronal chloride cotransporters affecting the inhibitory neurotransmission (Campbell et al., 2015; Tewari et al., 2018). Together, these alterations result in greater susceptibility to

* Corresponding author.
** Corresponding author at: Department of Physiology and Pharmacology, Sapienza University, Laboratory affiliated to Istituto Pasteur Italia, Rome, Italy.
E-mail addresses: mariaamalia.dicastro@uniroma1.it (M.A. Di Castro), cristina.limatola@uniroma1.it (C. Limatola).
[1] Co-last authors

https://doi.org/10.1016/j.nbd.2022.105894
Received 22 March 2022; Received in revised form 7 October 2022; Accepted 10 October 2022
Available online 12 October 2022

epilepsy, neurodegeneration, and cognitive defects, common comorbidities of glioma (Lange et al., 2021). On the other hand, recent evidence demonstrated that the selective activation of fast-spiking interneurons by optogenetic technique in glioma-bearing mice reduced tumor cell proliferation, demonstrating that the glutamatergic and GABAergic inputs may have contrasting effects on glioma (Tantillo et al., 2020).

Environmental cues, such as sensory, motor, and social stimuli are reported to positively influence animal physiology and social behavior, modulating the brain microenvironment with effects on neuronal plasticity, learning, and memory (van Praag et al., 2000). Cellular and molecular modifications underlie the different effects of the enriched environment (EE): correlations have been identified among dendritic arborization, the number of spines in some cell populations, the increase in hippocampal neurogenesis, and the level of neurotrophins such as BDNF, VEGF and NGF (van Praag et al., 2000). Similarly, the EE-induced alterations of neuronal plasticity are due to increased expression of synaptic proteins and neurotransmitter receptors (Rampon et al., 2000; Mohammed et al., 2002; Nithianantharajah et al., 2004; Nithianantharajah and Hannan, 2006). Different studies investigated the effects of environmental stimulation on the visual cortex. The visual cortex consists of six layers, with layer IV receiving the majority of thalamic inputs, and transmitting visual information from the retina. Pyramidal neurons of the layers II-III receive inputs from layer IV and weave them with associational cortico-cortical connections. Interestingly, the primary visual cortex (V1) is a paradigmatic system for studying how brain structure is modified by environmental cues because in adulthood pyramidal neurons of layer II-III are particularly susceptible to experience-dependent synaptic modifications (Karmarkar and Dan, 2006; Sale et al., 2007; Maffei and Turrigiano, 2008). In particular, EE promotes the recovery of visual acuity in adult amblyopic rats via a reduction of intracortical inhibition, and, in mice, it extends into adulthood the sensitive period for ocular dominance plasticity (Sale et al., 2007; Beaulieu and Cynader, 1990a; Beaulieu and Cynader, 1990b; Baroncelli et al., 2010; Greifzu et al., 2014).

Housing in EE also influences the development of several diseases, including cancer. Psychosocial distress (negative stress) is associated with a higher incidence of cancer and a lower survival rate (Chida et al., 2008; Hamer et al., 2009), while eustress (positive stress) inhibits cancer development (Sanchis-Gomar et al., 2012). Housing mice in EE is a classic model of eustress used to study the effects of the environment (van Praag et al., 2000). Animals housed in an EE show reduced tumor growth in models of melanoma, colon, breast, and pancreatic cancer (Cao et al., 2010; Nachat-Kappes et al., 2012; Li et al., 2015). We previously reported that in a glioma-bearing mouse model, EE exposure counteracts the growth of glioma injected in the striatum through the promotion of the anti-inflammatory phenotype of microglia (Garofalo et al., 2015; Garofalo et al., 2017). However, the electrophysiological changes underlying the effects of EE on tumor brain have been poorly explored.

In the present study, we injected syngeneic glioma in the V1 of C57BL/6 mice and investigated the alterations of synaptic transmission in pyramidal neurons of layer II/III. We found that glioma-bearing mice have reduced excitatory and inhibitory synaptic transmission in this region and that this deficit was partially rescued in mice housed in EE.

2. Materials and methods

2.1. Mice and cell line

Experiments described in the present work were approved by the Italian Ministry of Health in accordance with the guidelines on the ethical use of animals from the European Community Council Directive of September 22, 2010 (2010/63/EU), the Italian D. Leg. 26/2014. All possible efforts were made to minimize animal suffering and to reduce the number of animals used per condition by calculating the necessary sample size before performing the experiments. We used two-month-old male C57BL/6 (WT) mice from Charles River Laboratories. Mice were housed in standard breeding cages at a constant temperature (22 ± 1 °C) and relative humidity (50%). Food and water were available ad libitum. The GL261 glioma cell line (RRID:CVCL Y003) (kindly provided by Prof. Michela Matteoli, Humanitas, Milan, Italy) was cultured in DMEM supplemented with 20% heat inactivated FBS, 100 IU/ml penicillin G, 100 mg/ml streptomycin, 2.5 mg/ml amphotericin B, 2 mM glutamine, and 1 mM sodium pyruvate.

2.2. Environmental enrichment

Male mice were housed for 5 weeks in EE: 10 mice for cage (36 cm × 54 cm × 19 cm) in the presence of an assortment of objects, including climbing ladders, seesaws, running wheels, balls, plastic and wood objects suspended from the ceiling, paper, cardboard boxes and nesting material. Toys were changed every 2 days, and the bedding every week. Control SE mice were in pairs, in standard cages: 30 cm × 16 cm × 11 cm. Both the EE and SE groups received chow and water ad libitum, on a 12-h light/dark cycle.

2.3. Intracranial injection of glioma

Male C57BL/6 mice were anesthetized with Zoletil (40 mg/kg) and Rompun (10 mg/kg, i.p.) and placed in a stereotaxic head frame. Animals were injected with 4×10^4 GL261 cells using a stereotaxic apparatus: a median incision of ~1 cm was made, a burr hole was drilled in the skull, and cells were injected 2.8 mm lateral (right) and 0.3 mm anterior to the lambda in the right V1 area. Cells were suspended in PBS (2 ml) and injected with a Hamilton syringe at a rate of 1 ml/min at 0.95 mm depth. After 17 days, animals were sacrificed for different analyses.

2.4. Immunostaining

Seventeen days after injection of glioma cells, mice were overdosed with chloral hydrate (400 mg/kg, i.p.) and then intracardially perfused with PBS; brains were then isolated and fixed in 4% formaldehyde and snap frozen. Cryostat sections (20 mm) were washed in PBS, blocked (3% goat serum in 0.3% Triton X-100) for 1 h at RT, and incubated overnight at 4 °C with specific antibodies diluted in PBS containing 1% goat serum and 0.1% Triton X-100. The sections were incubated with anti-Ki67 (1:200). After several washes, sections were stained with the corresponding fluorophore-conjugated antibodies (Alexa-fluor, Invitrogen; 1:1000) and Hoechst (Cell Signaling Technology Cat# 4082, RRID:AB_10626776; 1:2000) for nuclei visualization and analyzed using a fluorescence microscope.

2.5. Image acquisition and data analysis

Images were digitized using a CoolSNAP camera (Photometrics) coupled to an ECLIPSE Ti—S microscope (Nikon) and processed using MetaMorph 7.6.5.0 image analysis software (Molecular Devices). Brain slices were scanned by consecutive fields of vision (10× objective lens) to build a single image per section. The percentage of positive cells was measured as the ratio of the area occupied by fluorescent cells versus the total tumor area (by converting pixels to square millimeters). At least 12 coronal sections per brain around the point of injection were analyzed for comparison between different treatments.

2.6. Slice preparation for electrophysiology

Animals anesthetized with isoflurane were decapitated and the whole brains were rapidly removed from the skull and immersed for 10 min in ice-cold gassed (95% O_2, 5% CO_2), sucrose-based artificial cerebrospinal fluid (ACSF) containing (in mM) 87 NaCl, 63.5 Sucrose, 2 KCl, 7 $MgCl_2$, 0.5 $CaCl_2$, 25 $NaHCO_3$, 1.2 NaH_2PO_4 and 10 glucose, pH

7.4, 300–305 mOsm, then sectioned (ThermoScientific HM 650 V) in coronal slices (300 μm). After their preparation, slices were allowed to recover for at least 1 h at 30 °C in ACSF containing NaCl 125 mM, KCl 4 mM, $CaCl_2$ 2.5 mM, $MgSO_4$ 1.5 mM, NaH_2PO4 1 mM, $NaHCO_3$ 26 mM, glucose 10 mM; 295–300 mOsm for field recordings and in NaCl 125, KCl 2, $CaCl_2$ 2, $MgCl_2$ 1.2, NaH_2PO_4 1.2, $NaHCO_3$ 25, glucose 10 for patch clamp recordings. Electrophysiological recordings were performed in layers II/III of the primary visual cortex (V1). In glioma bearing slices, the pipette for whole-cell recordings was positioned approximately 100–150 μm from the border of the tumor (Fig. 2). For field excitatory post-synaptic potential, the recording pipette was located around 300–500 μm from the tumor edge.

2.7. Patch-clamp recordings

Whole-cell patch-clamp recordings were performed from layer II/III pyramidal neurons (Fig. 2) at room temperature by using a Multiclamp 700B amplifier (Molecular Devices, USA). The ACSF (composition in mM: NaCl 125, KCl 2, $CaCl_2$ 2, $MgCl_2$ 1.2, NaH_2PO_4 1.2, $NaHCO_3$ 25, glucose 10) was perfused at a rate of approximately 2 ml/min by using a gravity-driven perfusion system. Cell capacitance was constantly monitored over time and experiments where access resistance changed more than 20% were discarded. Glass electrodes (3–4 MΩ) were pulled with a vertical puller (PC-10, Narishige). Pipettes were filled with 135 mM Cs Methanesulfonate, 10 mM Hepes, 0.5 mM EGTA, 2 mM Mg-ATP, 0.3 mM Na_3-GTP, and 2 mM $MgCl_2$ (295–300 mOsm, pH 7.2). Spontaneous excitatory post-synaptic currents (sEPSCs) were recorded by holding the cell at the reversal potential of GABA current (−65 mV). Spontaneous inhibitory currents were recorded at the reversal potential of glutamatergic currents (0 mV). Signals were acquired (sampling 10 kHz, low-pass filtered 2 kHz) with DigiData-1440A using pCLAMP-v10 software (Molecular Devices, USA).

Passive properties of the cells were calculated by applying a 10 mV hyperpolarizing voltage square pulse delivered from −65 mV holding potential. Membrane capacitance was estimated as the total charge (i.e., the current integral, Qstep) mobilized in each cell by a 10 mV hyperpolarizing step (Vstep): Qstep/Vstep. The input resistance, Rin, was measured from the same protocol at the end of a 30 ms pulse, when the current trace reached the steady state.

2.8. Spontaneous synaptic currents identification

In the preprocessing phase baseline, drifts were removed by subtracting from the original recording the output of a median sliding 300 ms window filter. High-frequency artifacts were then removed by low pass filtering the traces with passband frequency at 1 kHz. The detection of spontaneous post-synaptic currents (sPSCs) has been performed following a semi-automatic template fit algorithm proposed by (Pernía-Andrade et al., 2012). Briefly, a 'template event' $\mathbf{x(t)}$ of post-synaptic currents was extracted for each recording separately. The template was computed by averaging the events between $[\mathbf{t^* - 10; t^* + 20}]$ ms crossing a threshold at time $\mathbf{t^*}$. The threshold was set to the 99th percentile in a sliding window of length 2 s.

The w(t) trace was fit (*fminsearch* in Matlab) to the sum of a double exponential as follows:

$$\widetilde{\mathbf{w}}(\mathbf{t}) = \frac{\mathbf{A}}{\mathbf{A}'}\left[-\mathbf{e}^{-\frac{\mathbf{t}}{\tau_r}} + \mathbf{e}^{-\frac{\mathbf{t}}{\tau_d}}\right] \quad (1)$$

where $\mathbf{A}' = \frac{\tau_r}{\tau_d}\frac{\tau_r}{\tau_r - \tau_d}$, $\mathbf{A}$ is the peak amplitude of w(t), $\boldsymbol{\tau_r}$ is the rise and $\boldsymbol{\tau_d}$ is the decay time.

Once the fit $\widetilde{\mathbf{w}}(\mathbf{t})$ of the template synaptic event is determined the algorithm proceeds as follows: (i) the recorded trace is deconvolved from the template $\widetilde{\mathbf{w}}(\mathbf{t})$; (ii) the all-point-histogram of the deconvolved trace is fit to a Gaussian distribution and a threshold value (4 to 5 times the distribution standard deviation) is chosen; (iii) the deconvolution trace $\mathbf{y(t)}$ is then scanned for local maxima, which are defined as those sample points fulfilling the criterion $\mathbf{y(i-2) < y(i-1) < y(i) > y(i+1) > y(i+2)}$.Such local maxima correspond to the onset of the sPSC in the original recording. Artifactual synaptic events detected by the algorithm were manually discarded by further analysis.

2.9. Parameters of sPSC

Each synaptic event was fitted to the sum of a double exponential, as in eq. (1), and subtracted from the recording. This operation allowed for a better fitting of the segmented trace in case the onset times of two (or more) following detected events were less than 2 times the decay time of the preceding one(s). From each fitted waveform we extracted: (i) the peak amplitude; (ii) the decay time; (iii) the rise time and the inter-event interval (IEI). The frequency rate of the synaptic events was computed as the ratio between the number of detected events and the recording length in seconds.

2.10. Evoked current recordings

A concentric bipolar stimulating electrode (SNE-100 × 50 mm long Elektronik-Harvard Apparatus GmbH, Crisel Instruments, Rome, Italy) was positioned in layer IV to evoke EPCSs and IPSCs from layer II/III neurons clamped respectively at −65 mV and 0 mV. Stimuli of increased intensity were applied every 20 s. Stimulus intensity was delivered through an A320R Isostim Stimulator/Isolator (WPI). The amplitude of each EPSC/IPSC was measured relative to a 2 ms long baseline period starting 3 ms before stimulation. The evoked E/I ratio was calculated in each cell at the maximal stimulation intensity of both I—O curves (stable E/I ratio).

2.11. Field excitatory post synaptic potential (fEPSP) recordings

Slices were transferred to the slice-recording chamber interface (BSC1, Scientific System Design Inc), maintained at 30–32 °C and constantly superfused at the rate of 2.5 ml/min with oxygenated ACSF. At the beginning of each recording, a concentric bipolar stimulating electrode (SNE-100X 50 mm long Elektronik–Harvard Apparatus GmbH) was placed in layer IV of primary visual cortical slices. Stimuli consisted of 100 μs constant current pulses of variable intensities, applied at 0.05 Hz. A glass micropipette (0.5–1 MΩ) filled with ACSF was placed in the layer II/III pyramidal neurons (Fig. 3A). Stimulus intensity was adjusted to evoke fEPSP of about 50% of the maximal amplitude. Evoked responses were monitored online and stable baseline responses were recorded for at least 10 min. Only the slices that showed stable fEPSP amplitudes were included in the experiments. The paired-pulse ratio (PPR) was measured from responses to two synaptic stimuli spaced by 50, 70, 100, 150 or 200 ms. PPR was calculated as the ratio between the fEPSP amplitude evoked by the second stimulus (A2) and that by the first (A1; A2/A1). fEPSPs were recorded and filtered (low pass at 1 kHz) with an Axopatch 200A amplifier (Axon Instruments, CA) and digitized at 10 kHz with an A/D converter (Digidata 1322A, Axon Instruments). Data acquisition was stored on a computer using pClamp 9 software and analyzed offline with Clampfit 10 software (both from Axon Instruments).

2.12. Statistical analysis

For electrophysiological experiments, statistical significance was assessed by two-way ANOVA (ANOVA2) for parametrical data and two-way ANOVA on ranked for non-parametric data considering environmental caging conditions and the presence/absence of glioma, as the between-subject variables. Normality was verified with the Saphiro-Wilk test. Post hoc comparisons were performed with the Dunn-Sidak test.

For the cumulative distribution analyses, we applied the

Kolmogorov-Smirnov two-sample test (KS). A pairwise two-sample KS test was used to determine whether the distributions of amplitude and inter-event interval of spontaneous events were significantly different i) between the environmental caging condition and ii) between the presence/absence of glioma. To prevent some cells (e.g., those recorded for longer periods or those with conspicuous spontaneous activity) to weight more on the KS test, we randomly extracted from each cell 200 consecutive parameter values prior to any statistical analysis. The alpha value for the KS test was set to $p = 0.05$ with post-hoc Bonferroni correction.

For Paired pulse ratio experiments and Input/output curves statistical significance was assessed by two Way Repeated Measures ANOVA. Post-hoc comparisons were performed with Fisher's test.

For tumor proliferation, statistical analyses were conducted using Student's *t*-test.

Sample size (n/N) refers to the number of: (i) slices/mice, for field cell recording analysis; (ii) cells/mice for patch clamp recordings. N refers to the number of mice for Ki67+ cells analysis. All data are expressed as mean ± standard error of the mean (SEM), or median ± SEM as stated.

3. Results

3.1. EE reduces tumor proliferation in primary visual cortex

We previously demonstrated that housing in EE reduces glioma growth and increases the survival of mice injected with glioma in the striatal region (Garofalo et al., 2015; Garofalo et al., 2017). Here, we investigated whether the anti-tumor effect of housing mice in an EE was maintained in different brain regions, such as V1. For this purpose, mice were housed for five weeks in standard environment (SE) or EE before glioma cell transplantation (Fig. 1A-B). Quantitative analysis of glioma cell proliferation, performed 17 days after the inoculation, showed that EE housing reduced the area covered by Ki67+ cells in the tumor mass compared to SE ($p = 0.035$) (Fig. 1C-D). These data show that, similarly to what was observed in other experimental conditions, exposure to an EE reduces tumor growth, supporting the beneficial role of environmental stimulation on different tumors and regions (Cao et al., 2010; Nachat-Kappes et al., 2012; Li et al., 2015; Garofalo et al., 2015; Garofalo et al., 2017).

3.2. Effects of EE on excitatory post-synaptic activity in peritumoral neurons

To investigate how EE impacts synaptic transmission in peritumoral neurons, we analyzed the spontaneous excitatory synaptic currents in visual cortical slices harvested from SE, EE and GL261-injected mice housed in standard (SE-G) or enriched environment (EE-G). We performed whole-cell patch-clamp recordings from layer II/III pyramidal neurons clamped at −65 mV (Fig. 2A-B). We found that both the environment and glioma had a main effect on averaged sEPSC frequency ($F = 5.57, p = 0.02$, $F = 4.16, p = 0.01$ respectively, ANOVA2) and post-hoc analysis revealed that EE increased the sEPSC frequency compared to SE ($p = 0.02$, Dunn-Sidak post-hoc test, Fig. 2C). The cumulative probability curve for IEIs was shifted towards the left in EE compared to SE mice ($p < 0.0001$, KS test, Fig. 2D), further demonstrating an increased frequency in EE.

In addition, we observed a rightward shift of the IEIs cumulative function in SE-G compared to SE ($p = 0.01$, KS test) suggesting a moderate reduction in the frequency of sEPSC due to glioma presence, less pronounced in the EE-G curve that was slightly shifted on the left compared to SE-glioma ($p < 0.001$, KS test, Fig. 2D).

Regarding the averaged sEPSC amplitude, we found only a main effect of glioma ($F = 8.13$, $p = 0.05$, ANOVA2, Fig. 2E), although the cumulative function was slightly shifted towards higher sEPSC amplitudes in EE compared to SE, ($p < 0.0001$, KS test, Fig. 2F), indicating that EE increased the amplitudes of events, while the SE-G curve was shifted to the left compared to SE, demonstrating a reduction of sEPSC amplitude due to the presence of glioma ($p = 0.0132$, KS test, Fig. 2F). The cumulative curve of EE-G was slightly shifted to the right compared to SE-G ($p < 0.0001$, KS test), indicating a partial recovery of sEPSC amplitude towards SE values (Fig. 2F).

The increase in both the amplitude and frequency of sEPSC in EE-housed animals is in line with the potentiation of the excitatory synaptic transmission mediated by EE (Mainardi et al., 2010; Malik and Chattarji, 2012). Data on cumulative functions demonstrate that in glioma-bearing mice the amplitude of sEPSC was slightly reduced and the enriched environment has a modest effect on both sEPSC frequency and amplitude to rescue them towards SE values.

Since alterations in the spontaneous post-synaptic currents could be ascribed to several pre- and post-synaptic mechanisms, including alterations in the firing properties of presynaptic neurons, modifications at the synaptic levels of glutamate release or alterations in the post-synaptic receptor's properties, we recorded miniature excitatory post-synaptic currents in presence of tetrodotoxin to block the action potential-dependent release of glutamate. We found that the environment has a main effect on the mEPSC frequency ($F = 4.59$, $p = 0.03$, ANOVA2, Fig. 2G), increasing the average in EE compared to SE ($p = 0.03$, Dunn-Sidak post hoc test), similarly to what observed in sEPSC. In addition, cumulative distribution curves revealed a shift towards shorter

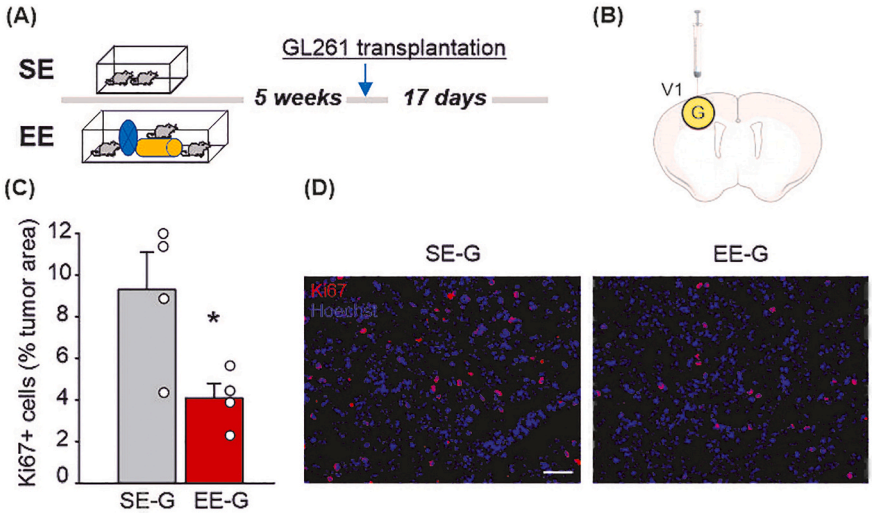

Fig. 1. EE exposure reduces glioma cell proliferation. A) Scheme of the experimental procedures for environmental enrichment. B) Representation of glioma injection in cortical visual cortex (V1). C) Quantification of Ki67+ cells (mean ± s.e.m. of Ki67+ area as % of the tumor area) 17 days after GL261 transplantation in mice housed in standard (SE-G) or enriched (EE-G) environment. SE: 9.31 ± 1.79%, EE: 4.08 ± 0.70%; $N = 4$ mice per condition, * $p = 0.035$, One-Way ANOVA). Representative immunofluorescences are shown on the right. Scale bar: 50 μm.

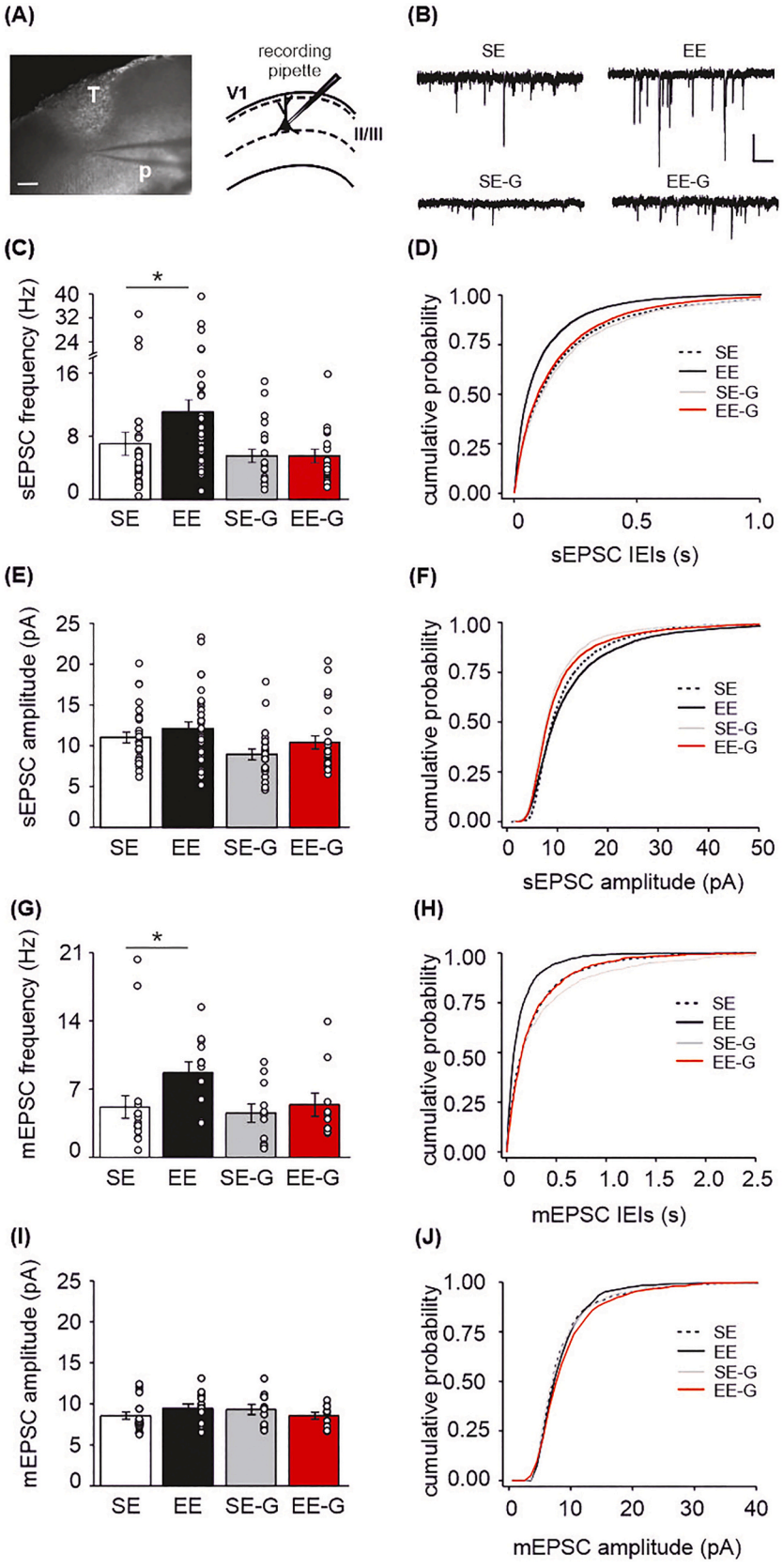

Fig. 2. Spontaneous excitatory currents are reduced by glioma and increased by housing in EE. A) Representative image of horizontal acute brain slice from a glioma-bearing mouse and schematic representation of pipette location for recordings. Tumor mass (T) is visible in layer I and II/III of the V1 cortex and patch pipette in the peritumoral area (P), scale bar: 150 μm. B) Examples of sEPSC traces recorded at −65 mV from standard-housed mice (SE), enriched-housed mice (EE), standard-housed glioma bearing mice (SE-G) and enriched-housed glioma bearing mice (EE-G). scale bars: 20 pA, 0.25 s. C) Mean frequency of sEPSC with single dots indicating the value for each cell in the group. SE: 7.05 ± 1.43 Hz, n/*N* = 28/9; EE: 11.09 ± 1.52 Hz, n/*N* = 32/11; SE-G: 5.52 ± 0.82 Hz, n/*N* = 22/10; EE-G: 5.51 ± 0.85 Hz, n/*N* = 24/10. D) Cumulative probability curves for IEIs (n. of events: SE = 5600, EE = 6400, SE-G = 4400, EE-G = 4600). E) Histogram of mean sEPSC amplitude (SE: 11.02 ± 0.67 pA, EE: 12.14 ± 0.79 pA, SE-G: 8.94 ± 0.67 pA, EE-G: 10.42 ± 0.81 pA) and corresponding cumulative probability functions in F). G) Histograms of mean values for mEPSC frequency (SE: 5.16 ± 1.15 Hz, n/*N* = 19/4; EE: 8.66 ± 1.12 Hz, n/*N* = 12/4; SE-G: 4.53 ± 0.95 Hz, n/*N* = 11/4; EE-G: 5.39 ± 1.19 Hz, n/*N* = 10/4). H) Cumulative distribution functions for mini IEIs (n. of events: SE = 1900, EE = 1200, SE-G = 1100, EE-G = 1000). J) Average of mEPSC amplitude (SE: 8.55 ± 0.42; Hz: EE: 9.42 ± 0.57 Hz; SE-G: 9.31 ± 0.61 Hz; EE-G: 9.35 ± 0.88 Hz) and corresponding cumulative curves in (J). (* $p \leq 0.01$).

IEIs in EE compared to the other groups ($p < 0.0001$, KS test, Fig. 2 H) and a shift towards longer IEIs in SE-G compared to both SE and EE-G ($p = 0.001$ and $p = 0.0001$ respectively, KS test, Fig. 2H) suggesting that glioma affects the action potential-independent excitatory transmission at the presynaptic level and that in EE the glioma effect was less pronounced.

Analysis of mEPSC amplitudes did not reveal differences in the mean values ($p = 0.08$, ANOVA2, Fig. 2I), as well as in the cumulative distribution function among all experimental groups (Fig. 2J). Overall, these data indicate that the increase in the frequency of both sEPSC and mEPSC in EE is related to presynaptic enhancement of spontaneous excitatory synaptic transmission.

Alterations in the frequency of spontaneous excitatory spontaneous synaptic transmission could result from several mechanisms including changes in the probability of neurotransmitter release, alterations in the firing of presynaptic fibers or modifications in the innervation of pyramidal neurons in layers II/III. Analysis of input resistance (Rin) and membrane capacitance did not reveal differences among all experimental groups indicating that environmental conditions and glioma did not affect the passive properties of pyramidal neurons, as reported by others (Supplementary Fig. 1) (Tewari et al., 2018).

To characterize the short-term plasticity, that estimates the presynaptic probability of release, we measured the plasticity of fEPSP responses to paired-pulse stimulations. A concentric bipolar stimulating electrode was placed in layer IV to record in layer II/III fEPSPs evoked by two consecutive stimuli at different interstimulus intervals (ISIs) namely, 50, 70, 100, 150, 200 ms (Fig. 3A-B). As previously reported, paired-pulse stimulation at layer II/III pyramidal synapses produces depression of the second response over the first (paired-pulse depression, PPD) that decreases with larger interstimulus-intervals (Varela et al., 1999). We confirm this behavior showing a gradual decrease of PPD along with the increase of ISIs (Fig. 3C). Two-Way repeated measures ANOVA analysis showed that there is a significant effect of experimental conditions ($p = 0.039$, $F = 2.890$), and ISIs ($p < 0.001$, $F = 159.595$, Fig. 3C) although no interaction between ISIs duration and conditions emerged. Multicomparison analysis showed that PPD in SE-glioma is reduced compared to SE mice (in particular, at 2 ISIs intervals: 100 and 200; $p < 0.05$). Interestingly, although no significant differences were observed between EE-G and SE-G in PPD, EE seems to rescue the reduction of PPD observed in SE-G, being the values of PPD in EE-G similar to SE conditions.

3.3. GABA inhibitory synaptic transmission in peritumoral neurons is affected by EE

A decrease in the number of GABAergic neurons with a concomitant reduction of the inhibitory tone has been described in the peritumoral cortex (Campbell et al., 2015). To investigate the effect of EE on inhibitory transmission in peritumoral neurons, we analyzed spontaneous GABAergic currents (sIPSCs) recorded at the reversal potential for glutamatergic currents (0 mV) from layer II/III pyramidal neurons.

We did not find any differences in the mean frequency and amplitude of sIPSCs among experimental groups. (Fig. 4B, D). Interestingly, although in standard conditions the cumulative function distribution showed that the EE had no effect on sIPSCs frequency, the presence of glioma shifted the IEIs cumulative curves towards longer values in SE-G, compared to SE ($p < 0.001$, KS test, Fig. 4C), indicating that glioma reduced the frequency of spontaneous inhibitory synaptic transmission in peritumoral neurons. The IEIs curve for EE-G mice, although slightly shifted to the left compared to SE-G ($p < 0.001$, KS test, Fig. 4C), does not reach SE values, indicating a partial recovery due to environmental stimulation. The cumulative function distribution of sIPSC amplitude (Fig. 4E) showed a mild rightward shift for EE compared to the SE ($p < 0.001$, KS test) suggesting that EE modestly potentiates the amplitude of spontaneous inhibitory events. The presence of glioma did not influence the amplitude of sIPSC in both SE and EE (Fig. 4 D, E).

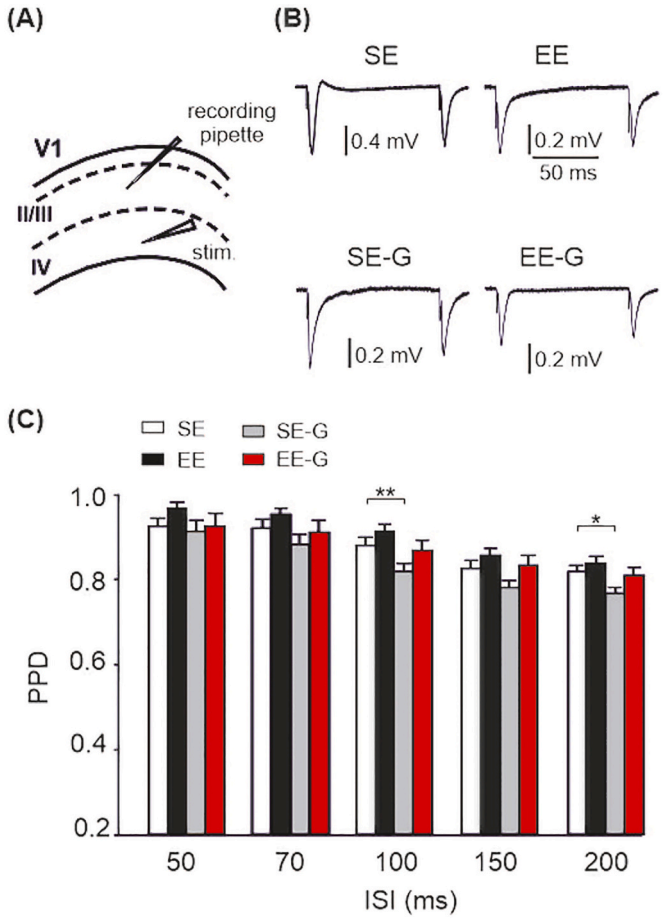

Fig. 3. Paired pulse ratio is altered by glioma in the standard-housing condition. A) Scheme of electrode positioning for field recordings of PPR. The bipolar electrode is located in layer IV, recording in layer II/III. B) Typical traces recorded at 100 ms of interstimulus interval (ISI) in the different conditions, as indicated. C) PPD measured at different interstimuli intervals (ISIs). Histograms of PPD at interstimulus of 50, 70, 100, 150, and 200 ms. The ordinates refer to an average value of PPD measured as a ratio between the second and the first fEPSP amplitude responses in V1 from SE (n/N = 25/5), EE (n/N = 24/5), SE-G (n/N = 30/9) and EE-G (n/N = 18/6), as indicated. * $p < 0.05$, ** $p < 0.01$, Two-way Repeated Measures ANOVA.

In recordings of miniature IPSC we found that glioma has a main effect on the frequency ($F = 5.73$, $p = 0.02$, ANOVA2), reducing it in SE-G compared to SE ($p = 0.02$, Dunn-Sidak post hoc test), while the environment does not significantly affect mIPSC frequency (Fig. 4F). The reduction in the SE-G frequency was also evident as a shift of the IEIs cumulative function to the right with respect to SE ($p < 0.0001$, KS test, Fig. 4G). Additionally, in Fig. 4G we observed that the IEIs curve of EE-G shifted to the right with respect to SE ($p = 0.0001$, KS test), unveiling that environmental stimulation reduced the frequency of miniature inhibitory events also in glioma-bearing mice ($p = 0.02$, KS test). By contrast, both the environment and glioma did not affect the mean values of mIPSC amplitudes and cumulative curves were similar between SE and SE-G, indicating that glioma reduced inhibition at the presynaptic level (Fig. 4 H, I). In EE and EE-G the mIPSC cumulative of amplitude was slightly shifted to the right, as observed in sIPSC, supporting a modest increase also in the amplitudes of inhibitory miniature events mediated by the environmental stimulation ($p = 0.007$ and $p < 0.001$ respectively, KS test, Fig. 4I).

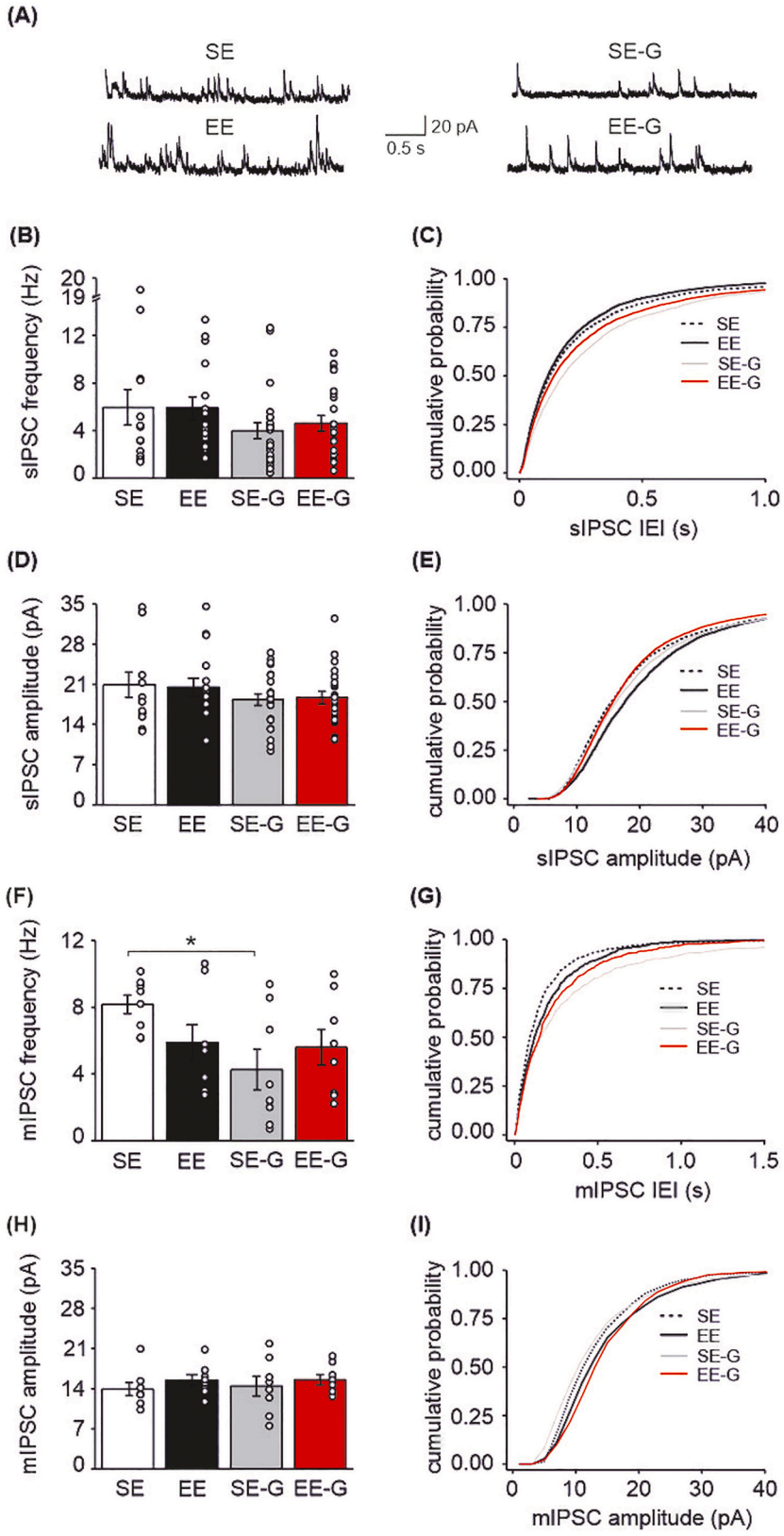

Fig. 4. Glioma reduced the frequency of spontaneous inhibitory synaptic transmission in peritumoral neurons. A) Example traces for sIPSC recorded at holding potential of 0 mV. Vertical bars = 30 pA, horizontal bar: 0.25 s. B) Mean amplitude of sIPSC. SE: 20.86 ± 2.18 pA, n/*N* = 13/7; EE: 20.41 ± 1.59 pA, n/*N* = 16/8; SE-G: 18.27 ± 1.01 pA, n/*N* = 23/10, EE-G: 18.61 ± 1.01 pA, n/*N* = 22/10. Single dots indicate the mean for each cell in the group. C) Cumulative function for sIPSC ampitudes in SE (2600 events), EE (3200 events), SE-G (4600 events), EE-G (4400 events) experimental groups. D) Average of the sIPSC frequency. SE: 5.96 ± 1.49 Hz; EE: 5.91 ± 0.93 Hz; SE-G: 3.99 ± 0.68 Hz; EE-G: 4.61 ± 0.6 Hz. E) Cumulative probability curves for IEIs in SE (2600 events), EE (3200 events), SE-G (4600 events) and EE-G (4400 events). F) Histograms of mean values for miniature IPSCs (SE: 13.92 ± 1.14 pA, n/*N* = 9/3; EE: 15.50 ± 0.96 pA, n/N = 9/3; SE-G: 14.44 ± 1.70 pA, n/*N* = 8/3, EE-G: 15.54 ± 0.92 pA, n/N = 8/3) and corresponding cumulative functions in I). H) Means of mIPSC frequency in SE (8.16 ± 0.55 Hz), EE (5.87 ± 1.07 Hz), SE-G (4.25 ± 1.22 Hz) and EE-G (5.59 ± 1.06 Hz). I) Cumulative probability curves of IEIs. * $p < 0.05$.

3.4. The evoked neurotransmission is impaired in peritumoral neurons and rescued by EE

We investigated the effect of housing in EE on the alterations in evoked transmission induced by glioma. We recorded evoked synaptic currents from pyramidal neurons in layers II/III at increasing stimulus intensities by changing the reversal potential from −65 mV to 0 mV to alternatively measure eEPSC and eIPSC (Fig. 5). Comparison of the input/output curve for excitatory responses in different conditions, performed by using Two-Way Repeated Measures ANOVA, showed no

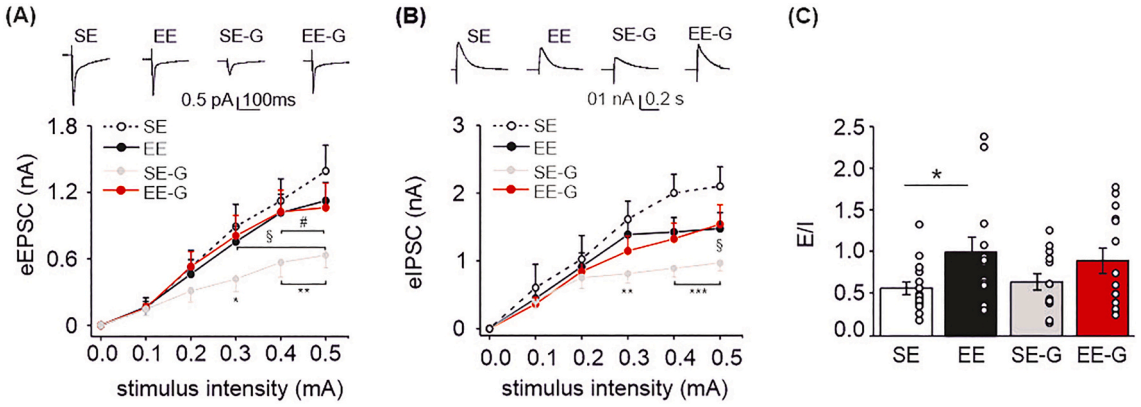

Fig. 5. EE rescues the reduction in the evoked neurotransmission in peritumoral neurons. A) On top, representative traces of eEPSC recorded at −65 mV in different experimental conditions, as indicated. On bottom, input-output curves of EPSC evoked at increasing stimulation intensities from different experimental groups: SE (n/*N* = 14/8), EE (n/*N* = 15/8), SE-G (n/N = 14/8) and EE-G (n/*N* = 18/10). ** p < 0.001 SE-G vs SE, § *p* < 0.05 SE-G vs EE, # p < 0.05 SE-G vs EE-G. B) On top, representative traces of eIPSC at 0 mV, as indicated. Input-output relationships of evoked IPSC (* p < 0.05 SE vs EE, ** *p* < 0.01 SE-G vs SE. C) The balance between excitation and inhibition (E/I ratio) was measured from responses evoked at maximal stimulation intensity. SE: 0.61 ± 0.15, n/N = 14/8; EE: 1.10 ± 0.16, n/N = 15/8; SE-G: 0.64 ± 0.14, n/*N* = 16/8; EE-G: 0.90 ± 0.13, n/N = 18/10. * *p* = 0.030.

effect of the experimental conditions (F = 1.900, *p* = 0.144) but a significant effect of stimulation (F = 99.709, *p* < 0.001) and of the interaction (F = 2.138, *p* = 0.009). Multiple comparison tests showed that the I/O curve of eEPSC in EE mice was similar to SE (*p* > 0.2 at each stimulation intensity, Fig. 5A) indicating that environmental enrichment did not alter evoked EPSC per se. In SE-G mice, currents evoked at higher intensities of stimulation were reduced compared to SE (0.3 mA *p* = 0.014; 0.4 mA *p* = 0.004; 0.5 mA p = 0.004) and EE (0.4 mA *p* = 0.019; 0.5 mA *p* = 0.03, Fig. 5A) indicating a reduction in excitatory synaptic strength. Interestingly, in EE-G mice, eEPSC amplitudes were similar to SE and EE and higher compared to SE-G (0.3 mA *p* = 0.024, 0.4 mA *p* = 0.015, 0.5 mA *p* = 0.037, Fig. 5A). These results indicate that EE induces a recovery of evoked excitatory synaptic transmission in glioma bearing mice housed in EE.

Two-Way Repeated Measures ANOVA for eIPSC revealed that there is a significant effect only of the stimulation (F = 63.545, p < 0.001) but not of the experimental conditions or of the interaction. Post-hoc comparison showed that input/output curves of eIPSC in SE-G mice were reduced compared to SE mice (0.3 mA, *p* = 0.001; 0.4 mV, *p* < 0.001; 0.5 mV, p < 0.001, Fig. 5B). We also confirm that EE reduced the amplitude of eIPSC compared to SE, as already reported (Sale et al., 2007; Greifzu et al., 2014) (0.4 mA, *p* = 0.05; 0.5 mA, p = 0.019, Fig. 5B). Interestingly, the EE-G group was statistically different from SE-G at higher stimulation intensity (0.5 mA, *p* = 0.045), also indicating a recovery of the inhibition in eIPSC mediated by EE.

In cortical neurons the prevailing view is that the balance between excitation and inhibition (E/I) is maintained across a critical value by homeostatic mechanisms that affect inhibitory and excitatory strength in response to changes in excitation (Froemke, 2015). To investigate whether the E/I balance is modulated by EE in the context of glioma, we measured the E/I ratio at the maximal stimulation intensity, where currents reached the plateau (0.5 mV). We found a main effect of the environment (F = 6.757, *p* = 0.012) but not of the tumor and interaction. In particular, the results in Fig. 5C show that EE increased the E/I ratio compared to SE, as expected because of the reduction in IPSC reported above (*t* = 0.482, p = 0.024). In SE-G mice E/I ratio was similar to SE (*t* = 0.456, *p* = 0.502, Fig. 5C) due to the concomitant reduction in both EPSC and IPSC. The EE-G group shows intermediate values of E/I, with no difference among SE-G and EE, in line with the partial recovery of eIPSCs (*t* = 0.2519, *p* = 0.183 and *t* = 0.101, *p* = 0.591, Fig. 5C).

4. Discussion

In this study we selected the layer II-III pyramidal neurons of the primary visual cortex, extensively modulated by sensory experience (Karmarkar and Dan, 2006; Sale et al., 2007; Maffei and Turrigiano, 2008), to investigate the neuronal changes induced by the presence of glioma, and the effects of environmental stimulation in counteracting these alterations. We showed that the presence of glioma reduces both the excitatory and inhibitory transmission in the peritumoral area. Furthermore, we extended previous findings in the striatum showing that glioma in the visual cortex is susceptible to EE that reduces tumor cell proliferation (Garofalo et al., 2015; Garofalo et al., 2017). The environmental stimulation potentiates spontaneous excitatory neuronal transmission, while reduces the evoked inhibitory currents, overall shifting the excitation-inhibition balance towards excitation. We found that in glioma-bearing mice housing in EE induces a recovery of tumor-mediated depression of evoked excitatory and inhibitory neuronal activity, while the effect on spontaneous transmission was less pronounced. Altogether, these data indicate that EE has a complex effect on synaptic transmission and that it can counteract the glioma-induced neuronal dysfunction particularly at the level of evoked neurotransmission, although other studies are warranted to identify underlying mechanisms in the interplay between environmental stimulation and glioma effect.

4.1. *Effects of EE on neuronal transmission*

Exposure to an EE induces several molecular and morphological alterations in the CNS, which are thought to underlie modifications in neuronal function and thus behavior (van Praag et al., 2000). The effects of EE have been studied in several cortical cerebral regions, such as the auditory cortex, the somatosensory cortex, and only to a limited extent in the visual cortex. In the auditory cortex, EE leads to increased excitatory post-synaptic current (EPSC) amplitudes and to increased PPD, indicating enhanced synaptic transmission (Nichols et al., 2007; Percaccio et al., 2005; Percaccio et al., 2007). EE has been reported to improve the x strength, threshold, selectivity, and latency of the responses in neurons of the auditory cortex (Percaccio et al., 2005; Engineer et al., 2004; Cai et al., 2009) and to promote the reorganization of the cortical tonotopic map (Noreña and Eggermont, 2006; Pienkowski and Eggermont, 2009; Zhu et al., 2011; Kim and Bao, 2013). However, some contradictory results are present in these studies, probably due to the different enrichment protocols, such as the duration and complexity

of the stimuli. In the visual cortex, EE has been reported to increase the neuronal responses to light enhancing visual acuity, stimulus contrast and temporal selectivity (Beaulieu and Cynader, 1990a; Beaulieu and Cynader, 1990b; Mainardi et al., 2010). Some studies were performed in models of monocular deprivation (MD) and amblyopia. MD performed during the critical period causes a robust shift in ocular dominance (OD) of neurons in V1, and a loss of spatial resolution (amblyopia) of the occluded eye. Housing mice in EE for 3 weeks reactivated OD plasticity in the adult visual cortex and recovered the visual acuity reducing the intracortical GABAergic inhibition and increasing the expression of BDNF (Sale et al., 2007; Baroncelli et al., 2010).

Here we analyze the effect of housing mice for 7 weeks in EE on the basal neurotransmission in V1. We report that EE strongly increases excitatory frequency of both sEPSC and mEPSC, whether the amplitude was enhanced only for sEPSC, indicating that the spontaneous excitatory synaptic transmission is potentiated by EE at the presynaptic level. Given that our data show that PPR is not modulated by EE, we can speculate that the increase in the spontaneous excitatory activity in EE could be ascribed to an increase in the firing of presynaptic neurons and/or an enhancement in the number of presynaptic contacts, the last being supported by the effect on the miniature EPSC recordings, where action potentials are blocked. On the spontaneous inhibitory transmission, we found that EE modestly increases the amplitude of both sIPSC and mIPSC but the frequency of mIPSC was reduced. While the last effect well reconciles with the reported reduction in GABA levels upon environmental stimulation (Sale et al., 2007; Mainardi et al., 2010), the increase of sIPSC and mIPSC amplitude goes in the opposite direction. One possibility is that the potentiation of the amplitude could be a compensatory mechanism to counterbalance the reduction in the GABA tone. Furthermore, we observed that EE has no effect on the excitatory evoked transmission, but reduced the inhibitory one, resulting in an overall net increase in the excitation/inhibition balance, as reported by other studies performed on the visual cortex (Sale et al., 2007; Greifzu et al., 2014). It is important to note that in our hand the effects of EE on spontaneous and evoked transmission differ and could reasonably be ascribed to specific regulatory mechanisms. Indeed, it has been demonstrated that diverse arrays of synaptic molecules selectively regulate synaptic vesicle's ability to fuse, so that vesicles released spontaneously can often be modulated independently from those that are released in response to stimulation (Rétaux et al., 1991; Scanziani et al., 1992; Kondo and Marty, 1998; Ramirez and Kavalali, 2011). Thus, we speculate that EE can modulate different synaptic molecules that in turn selectively regulate synaptic vesicles fusion leading to opposite effects on evoked and spontaneous transmission. Future experiments will be designed to assess mechanisms underlying the complex effects of environmental stimulation on neurotransmission.

4.2. Effects of glioma on neuronal transmission

The presence of glioma induces several modifications at the neuronal level. In particular, it has been reported that glioma cells release high amounts of glutamate via the system x(c)(−) (SXC), a cystine-glutamate anti-porter (Ye and Sontheimer, 1999). The impaired glutamate uptake in glioma cells and tumor-associated astrocytes contributes to increase the extracellular level of glutamate (Regehr, 2012,Campbell et al., 2020). Overstimulation of Ca^{2+} permeable NMDARs causes an uncontrolled Ca^{2+} increase in neurons surrounding glioma cells and mediates excitotoxic cell death and brain injury. Inhibitory transmission is also impaired by the presence of glioma. The reduction in the number of GABAergic neurons in the cortical area surrounding the tumor and in the expression levels of neuronal Cl^- cotransporter KCC2 which alters the intracellular level of Cl^-, produces a global GABAergic disinhibition in the peritumoral area (Campbell et al., 2015).

We here demonstrate that in the presence of glioma, the excitatory transmission is reduced, particularly the evoked post-synaptic currents recorded in the peritumoral neurons of cortical V1 and to a less extent the spontaneous one, including both sEPSC and mEPSC. This could be explained by a decrease in the circuit connectivity and loss of synapses induced by glutamate-mediated neuronal death (Ye and Sontheimer, 1999), supported by the evidence of a reduction in the frequency of miniature EPSC. Furthermore, we observed that glioma-bearing mice have a reduced PPD, suggesting an increased probability of glutamate release, in apparent contrast with a reduction of the evoked excitatory transmission. However, it is known that several pre- or post- synaptic mechanisms could specifically underlie short term synaptic depression, such as a reduced probability of synaptic release during the second stimulus, a depletion of the readily releasable pool or a desensitization of post-synaptic receptors (Regehr, 2012). Our data reveal that the amplitudes of mEPSC are not modified by glioma and allow us to exclude a post-synaptic site of effect. At the presynaptic site, it is possible that an altered Ca^{2+} dynamic in terminals surrounding the tumor could be responsible for the effect on PPD. Interestingly, at other sensory synapses, it has been demonstrated that a calcium-induced inhibition of voltage-gated calcium channels (VGCC) could depress calcium entry at the presynaptic terminal and reduce glutamate release, particularly at the second response during a PPR paradigm (Bellingham and Walmsley, 1999; Xu and Wu, 2005). We can speculate that calcium overload of terminals, due to excitotoxic level of glutamate in the vicinity of the tumor, could summate to the calcium entering at the pre-synapse following an action potential and accelerate the inactivation of VGCC, resulting in the major depression of the second response and reduction of PPD. In addition, the increased glutamate levels in glioma could activate presynaptic metabotropic receptors known to inhibit VGCC and depress glutamate release (Woodhall et al., 2007). In line with our observations, in layer V entorhinal neurons it has been shown that the activation of a specific group III mGluR depressed the amplitude of stimulus-evoked excitatory postsynaptic currents, with major effect on the second response during paired pulse stimulation, leading to a reduction of PPR (Billups et al., 2005). Lastly, we cannot exclude the fact that glioma-induced release of molecules related to inflammation could specifically affect different processes involved in neurotransmission.

Finally, as already reported (Campbell et al., 2012; Campbell et al., 2015), we confirmed a glioma-mediated reduction in the frequency of spontaneous inhibitory transmission (both sIPSC and mIPSC) and amplitude of evoked inhibitory currents, indicating a reduced GABAergic tone. The parallel reduction in both excitatory and inhibitory transmission observed in glioma-bearing mice leaves unaffected the overall E/I balance.

4.3. EE counteracts the effects of glioma

We demonstrate that EE counteracts some of the neuronal changes produced by glioma. In particular, EE rescues the reduction in the amplitudes of the evoked currents induced by the presence of glioma in the V1 area restoring the values to the control level. In addition, it also counteracts the reduction of PPD of excitatory transmission observed in glioma-bearing mice. However, EE has only a modest effect on excitatory spontaneous activity in glioma-bearing mice, less pronounced in inhibitory transmission. The reduction in tumor cell proliferation upon environmental stimulation suggests that EE could prevent neuronal alterations due to glioma-induced damage, as well as the decrease in circuit connectivity and loss of synapses, in turn ameliorating the evoked neuronal transmission. However, we cannot exclude that different sizes of the tumor in standard and enriched conditions can differently affect the electrical stimulation of presynaptic fibers during input-output experiments. Additionally, the effect of EE on neuronal transmission in glioma-bearing mice could be ascribed to the action of neurotrophic factors released upon EE stimulation, including BNDF that can modulate directly the excitatory and inhibitory transmission and counteract in a different manner the negative effects of glioma on neuronal transmission (Sale et al., 2007; Colucci-D'Amato et al., 2020; Guzikowski and Kavalali, 2022). This could also explain the discrepancy in the effect of EE on

spontaneous and evoked transmission in glioma-bearing mice, given that an opposite action of these mediators has been described for action potential dependent and independent neurotransmission. At last, other factors that could underlie the described EE impact, include the composition of the glioma microenvironment and the interplay between different cell types in the brain parenchyma. Further studies would be necessary to assess the specific effect of EE on glioma cells, possibly with transcriptomic and proteomic analysis to investigate specific molecular pathways. Pieces of evidence report that environmental stimulation affects microglial cell proliferation in a brain-region-specific manner (Ehninger and Kempermann, 2003; Ehninger et al., 2011). We have recently demonstrated that, in models of glioma, innate immune cells such as microglial and NK cells sense environmental signals and modify their phenotype towards a pro-inflammatory, antitumoral one (Garofalo et al., 2015; Garofalo et al., 2017). The ability of EE to act on cells of brain parenchyma to contrast glioma growth and proliferation could reduce tissue damage and cell death, and indirectly ameliorate neuronal functions. Although further studies are warranted to understand the mechanisms involved and to investigate the specific set of molecules involved in the regulation of spontaneous and evoked neurotransmission, this is to our knowledge the first report describing the effect of a generic EE stimulation on primary visual cortical neuronal transmission in a mouse model of glioma.

5. Conclusions

This study elucidates more in detail the electrophysiological changes underlying the effects of EE on tumor brain. Both excitatory and inhibitory synaptic transmission from peritumoral neurons were reduced. The exposure to an enriched environment induced a recovery from the tumor-mediated depression of both excitatory and inhibitory neuronal activities, in particular the evoked ones. Our data show that the environmental stimulation counteracts synaptic alterations induced by glioma and reduces tumor cell proliferation supporting EE as a useful therapy for glioma treatment.

Author contributions

C.L., conceptualization, funding acquisition, project administration, supervision, writing-original draft., M.C. conceptualization, funding acquisition, writing-review & editing. A.M. conceptualization, funding acquisition, formal analysis, writing-review & editing. M.A.D.C. conceptualization, data curation, investigation, formal analysis, writing-original draft, writing-review & editing. L.M. conceptualization, data curation, formal analysis, writing-original draft, writing-review & editing. S.G. investigation, fromal analysis, methodology. N.M. formal analysis, data curation, software, A.M. methodology. E.D.P. investigation, formal analysis, data curation, methodology. E.D.F. investigation, formal analysis, data curation, visualization. All authors contributed to the article and approved the submitted version.

Institutional review board statement

Experiments described in the present work were approved by the Italian Ministry of Health in accordance with the guidelines on the ethical use of animals from the European Community Council Directive of September 22, 2010 (2010/63/EU), the Italian D. Leg. 26/2014.

Data availability statement

The raw data supporting the conclusions of this article will be made available by the authors, without undue reservation.

Conflicts of interest

The authors declare no conflict of interest.

Data availability

Data will be made available on request.

Acknowledgments

S.G. is funded by AIRC (22329); C.L., A.M., M.C. are supported by PRIN2017. C.L. is also supported by AIRC2015/AIRC2019 (IG-16699 and IG-23010) and by the Italian Ministry of Health, Ricerca Finalizzata RF-2018-12366215. We thank Dr. Marco Mainardi for helpful suggestions in the design of experimental procedures; Eleonora Vannini for advices on protocol injection in V1. This paper is dedicated to the memory of our dear co-author Prof. Matteo Caleo, who passed away while this paper was being peer-reviewed. He contributed with enthusiasm and kidness by providing his strong expertise in neuronal plasticity processes of the visual cortex.

Appendix A. Supplementary data

Supplementary data to this article can be found online at https://doi.org/10.1016/j.nbd.2022.105894.

References

Baroncelli, L., Sale, A., Viegi, A., Maya Vetencourt, J.F., De Pasquale, R., Baldini, S., Maffei, L., 2010. Experience-dependent reactivation of ocular dominance plasticity in the adult visual cortex. Exp. Neurol. 226 (1), 100–109. https://doi.org/10.1016/j.expneurol.2010.08.009. Epub 2010 Aug 14. PMID: 20713044.

Beaulieu, C., Cynader, M., 1990a. Effect of the richness of the environment on neurons in cat visual cortex. I. Receptive field properties. Brain Res. Dev. Brain Res. 53 (1), 71–81. https://doi.org/10.1016/0165-3806(90)90125-i. PMID: 2350883.

Beaulieu, C., Cynader, M., 1990b. Effect of the richness of the environment on neurons in cat visual cortex. II. Spatial and temporal frequency characteristics. Brain Res. Dev. Brain Res. 53 (1), 82–88. https://doi.org/10.1016/0165-3806(90)90126-j. PMID: 2350884.

Bellingham, M.C., Walmsley, B., 1999. A novel presynaptic inhibitory mechanism underlies paired pulse depression at a fast central synapse. Neuron. 23 (1), 159–170. https://doi.org/10.1016/s0896-6273(00)80762-x.

Billups, B., Graham, B.P., Wong, A.Y., Forsythe, I.D., 2005. Unmasking group III metabotropic glutamate autoreceptor function at excitatory synapses in the rat CNS. J. Physiol. 565 (Pt 3), 885–896. https://doi.org/10.1113/jphysiol.2005.086736.

Buckingham, S.C., Campbell, S.L., Haas, B.R., Montana, V., Robel, S., Ogunrinu, T., Sontheimer, H., 2011. Glutamate release by primary brain tumors induces epileptic activity. Nat. Med. 17 (10), 1269–1274. https://doi.org/10.1038/nm.2453. PMID: 21909104; PMCID: PMC3192231.

Cai, R., Guo, F., Zhang, J., Xu, J., Cui, Y., Sun, X., 2009. Environmental enrichment improves behavioral performance and auditory spatial representation of primary auditory cortical neurons in rat. Neurobiol. Learn. Mem. 91 (4), 366–376. https://doi.org/10.1016/j.nlm.2009.01.005. Epub 2009 Jan 30. PMID: 19186213.

Campbell, S.L., Buckingham, S.C., Sontheimer, H., 2012. Human glioma cells induce hyperexcitability in cortical networks. Epilepsia. 53 (8), 1360–1370. https://doi.org/10.1111/j.1528-1167.2012.03557.x (Epub 2012 Jun 18. PMID: 22709330; PMCID: PMC3418468).

Campbell, S.L., Robel, S., Cuddapah, V.A., Robert, S., Buckingham, S.C., Kahle, K.T., Sontheimer, H., 2015. GABAergic disinhibition and impaired KCC2 cotransporter activity underlie tumor-associated epilepsy. Glia 63 (1), 23–36. https://doi.org/10.1002/glia.22730. Epub 2014 Jul 26. PMID: 25066727; PMCID: PMC4237714.

Campbell, S.C., Muñoz-Ballester, C., Chaunsali, L., Mills 3rd, W.A., Yang, J.H., Sontheimer, H., Robel, S., 2020. Potassium and glutamate transport is impaired in scar-forming tumor-associated astrocytes. Neurochem. Int. 133, 104628 https://doi.org/10.1016/j.neuint.2019.104628. Epub 2019 Dec 9. PMID: 31825815; PMCID: PMC6957761.

Cao, L., Liu, X., Lin, E.J., Wang, C., Choi, E.Y., Riban, V., Lin, B., During, M.J., 2010. Environmental and genetic activation of a brain-adipocyte BDNF/leptin axis causes cancer remission and inhibition. Cell. 142 (1), 52–64. https://doi.org/10.1016/j.cell.2010.05.029. PMID: 20603014; PMCID: PMC3784009.

Chida, Y., Hamer, M., Wardle, J., Steptoe, A., 2008. Do stress-related psychosocial factors contribute to cancer incidence and survival? Nat. Clin. Pract. Oncol. 5 (8), 466–475. https://doi.org/10.1038/ncponc1134. Epub 2008 May 20. PMID: 18493231.

Colucci-D'Amato, L., Speranza, L., Volpicelli, F., 2020. Neurotrophic factor BDNF, physiological functions and therapeutic potential in depression, neurodegeneration and brain cancer. Int. J. Mol. Sci. 21 (20), 7777. https://doi.org/10.3390/ijms21207777. PMID: 33096634; PMCID: PMC7589016.

Cuddapah, V.A., Robel, S., Watkins, S., Sontheimer, H., 2014. A neurocentric perspective on glioma invasion. Nat. Rev. Neurosci. 15 (7), 455–465. https://doi.org/10.1038/nrn3765. PMID: 24946761; PMCID: PMC5304245.

Daubon, T., Hemadou, A., Romero Garmendia, I., Saleh, M., 2020. Glioblastoma immune landscape and the potential of new immunotherapies. Front. Immunol. 11, 585616

https://doi.org/10.3389/fimmu.2020.585616. PMID: 33154756; PMCID: PMC7591769.
Ehninger, D., Kempermann, G., 2003. Regional effects of wheel running and environmental enrichment on cell genesis and microglia proliferation in the adult murine neocortex. Cereb. Cortex 13 (8), 845–851. https://doi.org/10.1093/cercor/13.8.845. PMID: 12853371.
Ehninger, D., Wang, L.P., Klempin, F., Römer, B., Kettenmann, H., Kempermann, G., 2011. Enriched environment and physical activity reduce microglia and influence the fate of NG2 cells in the amygdala of adult mice. Cell Tissue Res. 345 (1), 69–86. https://doi.org/10.1007/s00441-011-1200-z. Epub 2011 Jun 21. PMID: 21688212; PMCID: PMC3132349.
Engineer, N.D., Percaccio, C.R., Pandya, P.K., Moucha, R., Rathbun, D.L., Kilgard, M.P., 2004. Environmental enrichment improves response strength, threshold, selectivity, and latency of auditory cortex neurons. J. Neurophysiol. 92 (1), 73–82. https://doi.org/10.1152/jn.00059.2004. Epub 2004 Mar 10. PMID: 15014105.
Froemke, R.C., 2015. Plasticity of cortical excitatory-inhibitory balance. Annu. Rev. Neurosci. 38, 195–219. https://doi.org/10.1146/annurev-neuro-071714-034002 (Epub 2015 Apr 9. PMID: 25897875; PMCID: PMC4652600).
Garofalo, S., D'Alessandro, G., Chece, G., Brau, F., Maggi, L., Rosa, A., Porzia, A., Mainiero, F., Esposito, V., Lauro, C., Benigni, G., Bernardini, G., Santoni, A., Limatola, C., 2015. Enriched environment reduces glioma growth through immune and non-immune mechanisms in mice. Nat. Commun. 6, 6623. https://doi.org/10.1038/ncomms7623. PMID: 25818172; PMCID: PMC4389244.
Garofalo, S., Porzia, A., Mainiero, F., Di Angelantonio, S., Cortese, B., Basilico, B., Pagani, F., Cignitti, G., Chece, G., Maggio, R., Tremblay, M.E., Savage, J., Bisht, K., Esposito, V., Bernardini, G., Seyfried, T., Mieczkowski, J., Stepniak, K., Kaminska, B., Santoni, A., Limatola, C., 2017. Environmental stimuli shape microglial plasticity in glioma. Elife. 6, e33415 https://doi.org/10.7554/eLife.33415. PMID: 29286001; PMCID: PMC5774898.
Greifzu, F., Pielecka-Fortuna, J., Kalogeraki, E., Krempler, K., Favaro, P.D., Schlüter, O. M., Löwel, S., 2014. Environmental enrichment extends ocular dominance plasticity into adulthood and protects from stroke-induced impairments of plasticity. Proc. Natl. Acad. Sci. U. S. A. 111 (3), 1150–1155. https://doi.org/10.1073/pnas.1313385111. Epub 2014 Jan 6. PMID: 24395770; PMCID: PMC3903188.
Guzikowski, N.J., Kavalali, E.T., 2022. Nano-organization of spontaneous GABAergic transmission directs its autonomous function in neuronal signaling. Cell Rep. 40 (6), 111172 https://doi.org/10.1016/j.celrep.2022.111172.
Hamer, M., Chida, Y., Molloy, G.J., 2009. Psychological distress and cancer mortality. J. Psychosom. Res. 66 (3), 255–258. https://doi.org/10.1016/j.jpsychores.2008.11.002. Epub 2009 Jan 16. PMID: 19232239.
Jung, E., Alfonso, J., Osswald, M., Monyer, H., Wick, W., Winkler, F., 2019. Emerging intersections between neuroscience and glioma biology. Nat. Neurosci. 22 (12), 1951–1960. https://doi.org/10.1038/s41593-019-0540-y. Epub 2019 Nov 12. PMID: 31719671.
Karmarkar, U.R., Dan, Y., 2006. Experience-dependent plasticity in adult visual cortex. Neuron. 52 (4), 577–585. https://doi.org/10.1016/j.neuron.2006.11.001. Nov 22. PMID: 17114043.
Kim, H., Bao, S., 2013. Experience-dependent overrepresentation of ultrasonic vocalization frequencies in the rat primary auditory cortex. J. Neurophysiol. 110 (5), 1087–1096. https://doi.org/10.1152/jn.00230.2013. Epub 2013 Jun 5. PMID: 23741037; PMCID: PMC3763088.
Kondo, S., Marty, A., 1998. Differential effects of noradrenaline on evoked, spontaneous and miniature IPSCs in rat cerebellar stellate cells. J. Physiol. 509 (Pt 1), 233–243. https://doi.org/10.1111/j.1469-7793.1998.233bo.x. PMID: 9547396; PMCID: PMC2230957.
Lange, F., Hörnschemeyer, J., Kirschstein, T., 2021. Glutamatergic mechanisms in glioblastoma and tumor-associated epilepsy. Cells. 10 (5), 1226. https://doi.org/10.3390/cells10051226. PMID: 34067762; PMCID: PMC8156732.
Li, G., Gan, Y., Fan, Y., Wu, Y., Lin, H., Song, Y., Cai, X., Yu, X., Pan, W., Yao, M., Gu, J., Tu, H., 2015. Enriched environment inhibits mouse pancreatic cancer growth and down-regulates the expression of mitochondria-related genes in cancer cells. Sci. Rep. 5, 7856. https://doi.org/10.1038/srep07856. PMID: 25598223; PMCID: PMC4297951.
Maffei, A., Turrigiano, G.G., 2008. Multiple modes of network homeostasis in visual cortical layer 2/3. J. Neurosci. 28 (17), 4377–4384. https://doi.org/10.1523/JNEUROSCI.5298-07.2008. PMID: 18434516; PMCID: PMC2655203.
Mainardi, M., Landi, S., Gianfranceschi, L., Baldini, S., De Pasquale, R., Berardi, N., Maffei, L., Caleo, M., 2010. Environmental enrichment potentiates thalamocortical transmission and plasticity in the adult rat visual cortex. J. Neurosci. Res. 88 (14), 3048–3059. https://doi.org/10.1002/jnr.22461. PMID: 20722076.
Malik, R., Chattarji, S., 2012. Enhanced intrinsic excitability and EPSP-spike coupling accompany enriched environment-induced facilitation of LTP in hippocampal CA1 pyramidal neurons. J. Neurophysiol. 107 (5), 1366–1378. https://doi.org/10.1152/jn.01009.2011. Epub 2011 Dec 7. PMID: 22157122.
Mohammed, A.H., Zhu, S.W., Darmopil, S., Hjerling-Leffler, J., Ernfors, P., Winblad, B., Diamond, M.C., Eriksson, P.S., Bogdanovic, N., 2002. Environmental enrichment and the brain. Prog. Brain Res. 138, 109–133. https://doi.org/10.1016/S0079-6123(02)38074-9. PMID: 12432766.
Nachat-Kappes, R., Pinel, A., Combe, K., Lamas, B., Farges, M.C., Rossary, A., Goncalves-Mendes, N., Caldefie-Chezet, F., Vasson, M.P., Basu, S., 2012. Effects of enriched environment on COX-2, leptin and eicosanoids in a mouse model of breast cancer. PLoS One 7 (12). https://doi.org/10.1371/journal.pone.0051525 e51525. Epub 2012 Dec 13. PMID: 23272114; PMCID: PMC3521763.
Nichols, J.A., Jakkamsetti, V.P., Salgado, H., Dinh, L., Kilgard, M.P., Atzori, M., 2007. Environmental enrichment selectively increases glutamatergic responses in layer II/III of the auditory cortex of the rat. Neuroscience. 145 (3), 832–840. https://doi.org/10.1016/j.neuroscience.2006.12.061 (Epub 2007 Feb 8. PMID: 17291690; PMCID: PMC2824591).
Nithianantharajah, J., Hannan, A.J., 2006. Enriched environments, experience-dependent plasticity and disorders of the nervous system. Nat. Rev. Neurosci. 7 (9), 697–709. https://doi.org/10.1038/nrn1970. PMID: 16924259.
Nithianantharajah, J., Levis, H., Murphy, M., 2004. Environmental enrichment results in cortical and subcortical changes in levels of synaptophysin and PSD-95 proteins. Neurobiol. Learn. Mem. 81 (3), 200–210. https://doi.org/10.1016/j.nlm.2004.02.002. PMID: 15082021.
Noreña, A.J., Eggermont, J.J., 2006. Enriched acoustic environment after noise trauma abolishes neural signs of tinnitus. Neuroreport. 17 (6), 559–563. https://doi.org/10.1097/00001756-200604240-00001. PMID: 16603911.
Percaccio, C.R., Engineer, N.D., Pruette, A.L., Pandya, P.K., Moucha, R., Rathbun, D.L., Kilgard, M.P., 2005. Environmental enrichment increases paired-pulse depression in rat auditory cortex. J. Neurophysiol. 94 (5), 3590–3600. https://doi.org/10.1152/jn.00433.2005. Epub 2005 Aug 10. Erratum in: J Neurophysiol. 2006 Feb;95(2): 1293. PMID: 16093336.
Percaccio, C.R., Pruette, A.L., Mistry, S.T., Chen, Y.H., Kilgard, M.P., 2007. Sensory experience determines enrichment-induced plasticity in rat auditory cortex. Brain Res. 1174, 76–91. https://doi.org/10.1016/j.brainres.2007.07.062. Epub 2007 Aug 9. PMID: 17854780.
Pernía-Andrade, A.J., Goswami, S.P., Stickler, Y., Fröbe, U., Schlögl, A., Jonas, P., 2012. A deconvolution-based method with high sensitivity and temporal resolution for detection of spontaneous synaptic currents in vitro and in vivo. Biophys. J. 103 (7), 1429–1439. https://doi.org/10.1016/j.bpj.2012.08.039. Epub 2012 Oct 2. PMID: 23062335; PMCID: PMC3471482.
Pienkowski, M., Eggermont, J.J., 2009. Long-term, partially-reversible reorganization of frequency tuning in mature cat primary auditory cortex can be induced by passive exposure to moderate-level sounds. Hear. Res. 257 (1–2), 24–40. https://doi.org/10.1016/j.heares.2009.07.011. Epub 2009 Aug 6. PMID: 19647789.
Ramirez, D.M., Kavalali, E.T., 2011. Differential regulation of spontaneous and evoked neurotransmitter release at central synapses. Curr. Opin. Neurobiol. 21 (2), 275–282. https://doi.org/10.1016/j.conb.2011.01.007. Epub 2011 Feb 18. PMID: 21334193; PMCID: PMC3092808.
Rampon, C., Jiang, C.H., Dong, H., Tang, Y.P., Lockhart, D.J., Schultz, P.G., Tsien, J.Z., Hu, Y., 2000. Effects of environmental enrichment on gene expression in the brain. Proc. Natl. Acad. Sci. U. S. A. 97 (23), 12880–12884. https://doi.org/10.1073/pnas.97.23.12880. PMID: 11070096; PMCID: PMC18858.
Razavi, S.M., Lee, K.E., Jin, B.E., Aujla, P.S., Gholamin, S., Li, G., 2016. Immune evasion strategies of glioblastoma. Front. Surg. 3, 11. https://doi.org/10.3389/fsurg.2016.00011. PMID: 26973839; PMCID: PMC4773586.
Regehr, W.G., 2012. Short-term presynaptic plasticity. Cold Spring Harb. Perspect. Biol. 4 (7), a005702 https://doi.org/10.1101/cshperspect.a005702. PMID: 22751149; PMCID: PMC3385958.
Rétaux, S., Besson, M.J., Penit-Soria, J., 1991. Opposing effects of dopamine D2 receptor stimulation on the spontaneous and the electrically evoked release of [3H]GABA on rat prefrontal cortex slices. Neuroscience. 42 (1), 61–71. https://doi.org/10.1016/0306-4522(91)90150-m. PMID: 1677746.
Sale, A., Maya Vetencourt, J.F., Medini, P., Cenni, M.C., Baroncelli, L., De Pasquale, R., Maffei, L., 2007. Environmental enrichment in adulthood promotes amblyopia recovery through a reduction of intracortical inhibition. Nat. Neurosci. 10 (6), 679–681. https://doi.org/10.1038/nn1899. Epub 2007 Apr 29. PMID: 17468749.
Sanchis-Gomar, F., Garcia-Gimenez, J.L., Perez-Quilis, C., Gomez-Cabrera, M.C., Pallardo, F.V., Lippi, G., 2012. Physical exercise as an epigenetic modulator: eustress, the "positive stress" as an effector of gene expression. J. Strength Cond Res. 26 (12), 3469–3472. https://doi.org/10.1519/JSC.0b013e31825bb594. PMID: 22561977.
Scanziani, M., Capogna, M., Gähwiler, B.H., Thompson, S.M., 1992. Presynaptic inhibition of miniature excitatory synaptic currents by baclofen and adenosine in the hippocampus. Neuron. 9 (5), 919–927. https://doi.org/10.1016/0896-6273(92)90244-8. PMID: 1358131.
Tantillo, E., Vannini, E., Cerri, C., Spalletti, C., Colistra, A., Mazzanti, C.M., Costa, M., Caleo, M., 2020. Differential roles of pyramidal and fast-spiking, GABAergic neurons in the control of glioma cell proliferation. Neurobiol. Dis. 141, 104942 https://doi.org/10.1016/j.nbd.2020.104942. Epub 2020 May 11. PMID: 32423877.
Tewari, B.P., Chaunsali, L., Campbell, S.L., Patel, D.C., Goode, A.E., Sontheimer, H., 2018. Perineuronal nets decrease membrane capacitance of peritumoral fast spiking interneurons in a model of epilepsy. Nat. Commun. 9 (1), 4724. https://doi.org/10.1038/s41467-018-07113-0. PMID: 30413686; PMCID: PMC6226462.
van Praag, H., Kempermann, G., Gage, F.H., 2000. Neural consequences of environmental enrichment. Nat. Rev. Neurosci. 1 (3), 191–198. https://doi.org/10.1038/35044558. PMID: 11257907.
Varela, J.A., Song, S., Turrigiano, G.G., Nelson, S.B., 1999. Differential depression at excitatory and inhibitory synapses in visual cortex. J. Neurosci. 19 (11), 4293–4304. https://doi.org/10.1523/JNEUROSCI.19-11-04293.1999. PMID: 10341233; PMCID: PMC6782599.
Venkataramani, V., Tanev, D.I., Strahle, C., Studier-Fischer, A., Fankhauser, L., Kessler, T., Körber, C., Kardorff, M., Ratliff, M., Xie, R., Horstmann, H., Messer, M., Paik, S.P., Knabbe, J., Sahm, F., Kurz, F.T., Acikgöz, A.A., Herrmannsdörfer, F., Agarwal, A., Bergles, D.E., Chalmers, A., Miletic, H., Turcan, S., Mawrin, C., Hänggi, D., Liu, H.K., Wick, W., Winkler, F., Kuner, T., 2019. Glutamatergic synaptic input to glioma cells drives brain tumour progression. Nature. 573 (7775), 532–538. https://doi.org/10.1038/s41586-019-1564-x. Epub 2019 Sep 18. PMID: 31534219.
Venkatesh, H.S., Johung, T.B., Caretti, V., Noll, A., Tang, Y., Nagaraja, S., Gibson, E.M., Mount, C.W., Polepalli, J., Mitra, S.S., Woo, P.J., Malenka, R.C., Vogel, H., Bredel, M., Mallick, P., Monje, M., 2015. Neuronal activity promotes glioma growth

through neuroligin-3 secretion. Cell. 161 (4), 803–816. https://doi.org/10.1016/j.cell.2015.04.012 (Epub 2015 Apr 23. PMID: 25913192; PMCID: PMC4447122).

Venkatesh, H.S., Tam, L.T., Woo, P.J., Lennon, J., Nagaraja, S., Gillespie, S.M., Ni, J., Duveau, D.Y., Morris, P.J., Zhao, J.J., Thomas, C.J., Monje, M., 2017. Targeting neuronal activity-regulated neuroligin-3 dependency in high-grade glioma. Nature 549 (7673), 533–537. https://doi.org/10.1038/nature24014. Epub 2017 Sep 20. PMID: 28959975; PMCID: PMC5891832.

Woodhall, G.L., Ayman, G., Jones, R.S., 2007. Differential control of two forms of glutamate release by group III metabotropic glutamate receptors at rat entorhinal synapses. Neuroscience. 148 (1), 7–21. https://doi.org/10.1016/j.neuroscience.2007.06.002.

Xu, J., Wu, L.G., 2005. The decrease in the presynaptic calcium current is a major cause of short-term depression at a calyx-type synapse. Neuron. 46 (4), 633–645. https://doi.org/10.1016/j.neuron.2005.03.024.

Ye, Z.C., Sontheimer, H., 1999. Glioma cells release excitotoxic concentrations of glutamate. Cancer Res. 59 (17), 4383–4391. PMID: 10485487.

Zhu, H., Tang, X., Wei, W., Mustain, W., Xu, Y., Zhou, W., 2011. Click-evoked responses in vestibular afferents in rats. J. Neurophysiol. 106 (2), 754–763. https://doi.org/10.1152/jn.00003.2011. Epub 2011 May 25. PMID: 21613592.